AIAA JOURNAL
Vol. 49, No. 7, July 2011

Effects of Oxygen Content on Dielectric Barrier Discharge Plasma Actuator Behavior

G. I. Font,* C. L. Enloe,† J. Y. Newcomb,‡ A. L. Teague,‡ A. R. Vasso,‡ and T. E. McLaughlin§
U.S. Air Force Academy, Colorado Springs, Colorado 80840

DOI: 10.2514/1.J050450

Atmospheric pressure dielectric barrier discharge plasma actuators are experimentally investigated. The temporal force characteristics and dielectric surface charging are determined using interferometry and split electrode techniques. The experiments are conducted at atmospheric pressure in diminishing levels of oxygen content to investigate the effects of oxygen ions. The results show that the force production is dominated by oxygen ions down to a level of 2–5% oxygen content. Temporal force measurements show that the plasma accelerates the air twice during the bias cycle for all oxygen levels, including pure nitrogen. Surface charging measurements show that, for oxygen content levels above 5%, a positive voltage region builds up on the dielectric downstream of the actuator. In the absence of oxygen, no such buildup is observed. The temporal force production characteristics in the pure nitrogen discharge appear to be greatly affected by the dielectric surface charging. Finally, at a 20% oxygen content level, the majority of the force is produced by the actuator while the exposed electrode is negative. When all of the oxygen is removed, the majority of the force is produced while the exposed electrode is positive.

Nomenclature

C_1	=	capacitance
E_{Local}	=	electric field near the exposed electrode edge
K_1	=	calibration constant
R_1	=	resistance
$V_{\text{exposed electrode}}$	=	voltage at driven electrode
V_{net}	=	total voltage at the surface (includes polarization charge contribution)
V_{segment}	=	voltage measured at segmented electrode element
$V_{\text{surface charge}}$	=	voltage due to charge deposited on the surface

I. Introduction

PLASMA actuators are simple electronic devices that can impart a small amount of momentum to a fluid flow. They have been shown to be useful in modifying and controlling separated flows over airfoils and backward facing steps [1–4]. In recent years, much study has been devoted to improving their performance, expanding their operating envelopes, and exploring the interaction of the plasma with the flow [5–12]. A plasma actuator consists of two electrodes separated by a dielectric, as shown in Fig. 1.

The upper electrode is exposed to the environment, while the lower electrode resides below a dielectric. The two are typically displaced in the free stream direction. An oscillating voltage of thousands to tens of thousands of volts at a frequency varying from hundreds to tens of thousands of hertz is usually placed across the two electrodes. The result is the generation of a plasma above the buried electrode which imparts momentum to the flow. The strategy of modifying the flow with a plasma actuator has several advantages including robustness due to a lack of moving parts and speed of modulation due to its inherent electronic nature.

Presented as Paper 2010 at the 48th AIAA Aerospace Sciences Meeting, Orlando, FL, 4–7 January 2010; received 21 January 2010; revision received 16 December 2010; accepted for publication 8 February 2011.

*Professor, Department of Physics. Member AIAA.
†Professor, Department of Physics. Senior Member. AIAA.
‡Cadet, Department of Physics.
§Director, Aeronautics Research Center, Department of Aeronautics. Associate Fellow AIAA.

In an effort to improve their efficiency, the present study attempts to increase the understanding of the plasma actuator operation by measuring their temporal force and surface charging characteristics. Similar experiments were previously conducted [13–15] for a typical actuator in atmospheric pressure air. In the present study, the amount of oxygen in the air is decreased until the actuator is functioning in a pure nitrogen environment. It is hoped that this will shed more light on the role of the oxygen ions in the force production mechanisms of the plasma actuator. The paper is divided as follows: Sec. II will discuss the experimental setup for both the force and surface charging measurements. Section III will detail the results of the temporal force measurements. Section IV will present the results of the surface charging measurements. This is followed by the summary.

II. Experimental Setup

The temporal force measurements are conducted by placing a typical actuator on a weak torsional pendulum as shown in Fig. 2. A He–Ne (632.8 nm) laser is reflected off a mirror attached to the actuator and an interferometry technique (1.2 m path length) is used to measure minute deflections of the actuator. The time history of the deflections is, then, differentiated to obtain the velocity and acceleration of the actuator. These are used to infer the force imparted by the actuator plasma and to the actuator by the induced fluid flow. Measurements are reported for the regime where the deflection is sufficiently small that the force due to the actuator is still an order of magnitude or more larger than the force due to the torsional spring. The torsional spring, which provides a restoring torque of only 0.02 mN/rad, merely serves to establish a motionless equilibrium state from which the actuator's displacement can be measured as a function of time. Actuator driving voltages from 7–15 kV and driving frequencies from 150–200 Hz are used. The driving frequency is lower than the typical kilohertz range but was necessary to resolve the force in time. More details can be found in [13]. To vary the oxygen content, the entire actuator mount is placed inside a sealed, high-vacuum-compatible chamber where the appropriate mixture of oxygen and nitrogen and pressure can be controlled. The oxygen content is known to better than 0.003% or the equivalent of 3 parts in 100,000. The volume of the chamber is 0.034 m^3 and the pressure is maintained at 690 Torr, which is the atmospheric pressure at the altitude of the laboratory. The actuator used for the experiments is made from copper tape and 1 mm thick circuit board. The upper electrode is 12 mm wide, while the lower electrode is 25 mm wide. There is no gap between the electrodes.

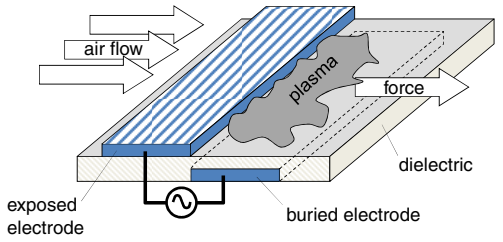

Fig. 1 Schematic of plasma actuator.

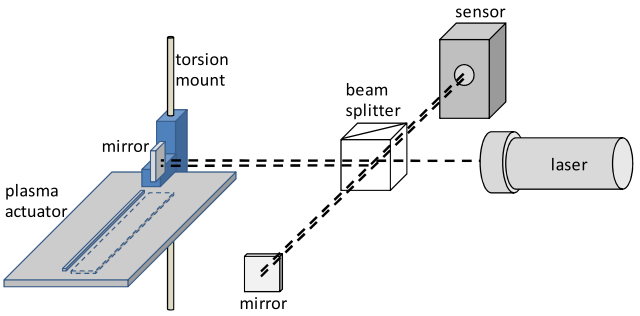

Fig. 2 Experimental setup for temporal force measurements.

In the second set of experiments, the surface charging on dielectric is measured. A portion of the actuator's lower electrode is cut into 12 segments, and each segment is isolated. The segments are small enough to give 1 mm resolution over the dielectric. The integrating circuit uses a 0.022 μF capacitor and a 50 MΩ resistor. An op-amp-based integrating circuit is placed from each segment to ground, as shown schematically in Fig. 3, allowing the displacement current to be measured at each location and the voltage profile on the surface to be determined.

The voltage (induced by the displacement current) at each segment has two contributions. The first is due to the charges on the exposed electrode, while the second is due to the charges on the surface. This gives

$$V_{\text{segment},i} = K_{1,i} V_{\text{exposed electrode}} + K_2 V_{\text{surface charge},i} \tag{1}$$

The segments, therefore, are calibrated in two steps. First, their response $K_{1,i}$ to a fluctuating voltage on the exposed electrode without plasma is measured. This is accomplished by keeping the voltage below the point where the plasma ignites. Second, the exposed electrode is temporarily extended above the buried electrode, to simulate charge on the surface, and the response K_2 of segments is again measured. One final calibration is necessary due to electric field lines that reach each segment from below the dielectric (C_3 on Fig. 3). This is calculated directly from Laplace's equation using the geometry and dielectric permittivity details of the actuator under study. This calibration $K_{3,i}$ varies from 1.0 at the edge of the exposed electrode to 0.0 at distances sufficiently far away. The net voltage at each location i of the upper surface of the dielectric is, therefore

$$V_{\text{net},i} = V_{\text{surface charge},i} + K_{3,i} V_{\text{exposed electrode}} \tag{2}$$

During the experiments, three measurements were made for each dielectric location. The results were then compiled and averaged to show the spatio-temporal charging evolution of the entire surface. More details about the experimental method are provided in [15].

III. Temporal Force Measurements

Force measurements were taken on a plasma actuator that was mounted on a torsional pendulum using interferometry techniques. The mounting structure was placed inside a sealed, high-vacuum-compatible chamber to control the oxygen/nitrogen ratio and the pressure. The oxygen content was varied from 20 to 0% and the average force was estimated by measuring the displacement. Three trials were conducted for each data point and the results were averaged. An actuation frequency of 200 Hz was used with an amplitude of 15 kV. The results for the average force normalized by the force produced in pure nitrogen are graphed in Fig. 4.

The force measurements indicate that the total momentum addition by the plasma actuator is proportional to the oxygen content above an oxygen concentration of 5%. Below this level, the relationship is more complex. As the oxygen content is decreased from 2% to zero, the force produced by the actuator declines slightly or remains constant within the error of the measurement. This agrees with previous results [16], which indicated that the plasma force was proportional to the O_2 content down to an oxygen level of 2–5%. The reason for oxygen dominance is due to the lower ionization potential of O_2 which results in oxygen ion production surpassing nitrogen ion production after a level of about 2%.

This is illustrated most clearly by Fig. 5 which displays the theoretical ratio of the ionization rates of oxygen and nitrogen as a function of the oxygen content and average electric field. The ionization rate constants used to calculate the data for this figure were obtained from [17]. For the current experiments, the field varies greatly over the dielectric, being greater near the exposed electrode and smaller farther away. However, the average field over the dielectric is roughly of the order of 1 MV/m. The theory shows that the rate of oxygen ionization should become greater than the rate of nitrogen ionization (rate O_2^+/rate $N_2^+ > 1.0$) at an oxygen content in the neighborhood of 2%. In the force measurements shown in Fig. 4, the point where the force becomes strongly dependent on the oxygen content (2–5% O_2 is the point where O_2^+ production becomes greater than the N_2^+ production. The theory also indicates a strong dependence on the average electric field. When the average field is near the breakdown voltage of air (3 MV/m), sufficient numbers of energetic electrons exist to efficiently ionize the nitrogen. This can be seen on the 3 MV/m line of Fig. 5, which does not show oxygen

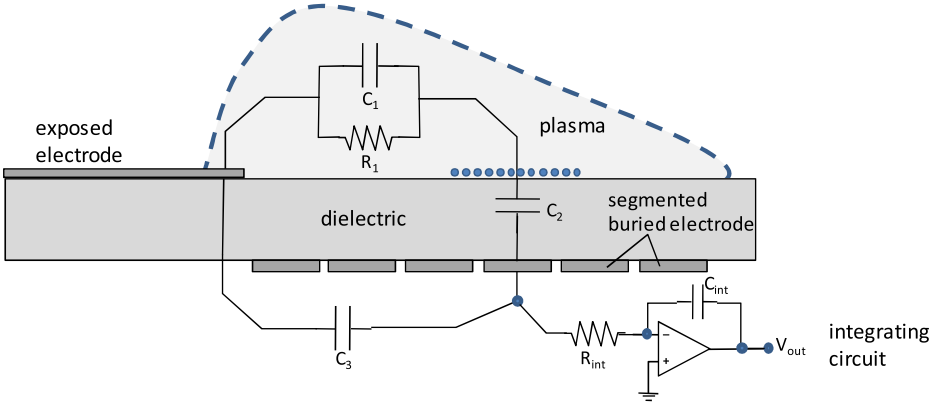

Fig. 3 Experimental setup for surface charging measurements.

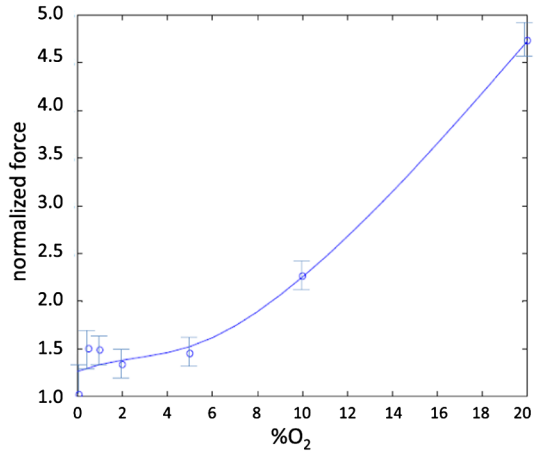

Fig. 4 Plasma actuator normalized force as a function of oxygen content.

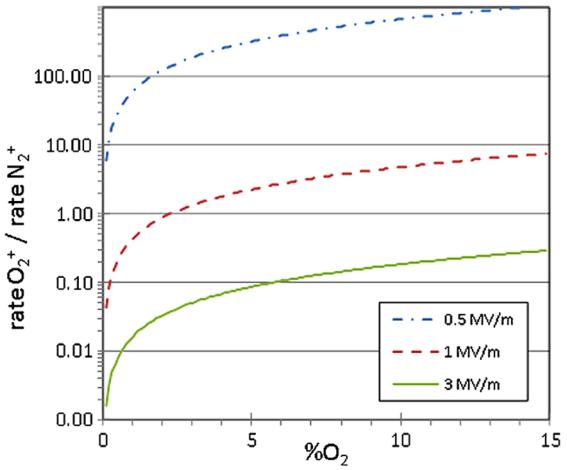

Fig. 5 Comparison of ionization rates of oxygen and nitrogen for various average electric fields.

ionization dominance even at 15% oxygen content. Conversely, if the average electric field is as little as 0.5 MV/m, only the oxygen can be efficiently ionized. On the graph, it can be seen that oxygen ionization dominates for the low electric field case even at 0.1% oxygen content.

Time-accurate deflection measurements of the plasma actuator were taken while varying the oxygen content for a driving frequency of 200 Hz. Figure 6 displays the measured driving voltage, plasma current, and the actuator velocity derived from the deflection data for the case with a 20% oxygen mixture. Further differentiation of the deflection measurements yield the acceleration and, by inference, the force. However, the acceleration data was excessively noisy. Therefore, the actuator velocity is displayed and its slope is used to infer the force applied by the actuator plasma and the force imparted by the air moving across it.

As expected, the plasma ignites twice during each AC voltage cycle; once while the exposed electrode is negative and once while it is positive. This can be seen in the current graph, which shows the current spikes from the microdischarges. For clarity, the plasma events (positive and negative) during a typical cycle are highlighted in the gray bands. We will concentrate on AC cycles after the third oscillation (time index larger than 0.02) because a few cycles are necessary, and sufficient, to establish repeatable effects from the plasma. From the graph of the actuator velocity, it is clear that while the driving voltage is negative going, the actuator feels a push from the plasma and accelerates. This accelerating force is thought to be due to the negative ions, which are being forced downstream by the negatively biased exposed electrode [11]. Following this, the actuator decelerates due to the viscous drag of the air [18]. When the plasma reignites, during the same AC cycle, the actuator accelerates again. This acceleration, however, is due to the positive ions being forced downstream. For the present voltage and frequency conditions, the second acceleration is small in comparison to the first acceleration. This is in agreement with previous studies [4,12,14]. The two accelerations can be seen more clearly during subsequent AC cycles.

The force pattern does not change as the oxygen content is diminished to 5%. As shown by Fig. 7, each of the plasma events during one bias cycle accelerates the actuator (and the air). The relative size of each acceleration does change, however. In the 20% oxygen case, the acceleration due to the negative ions was much

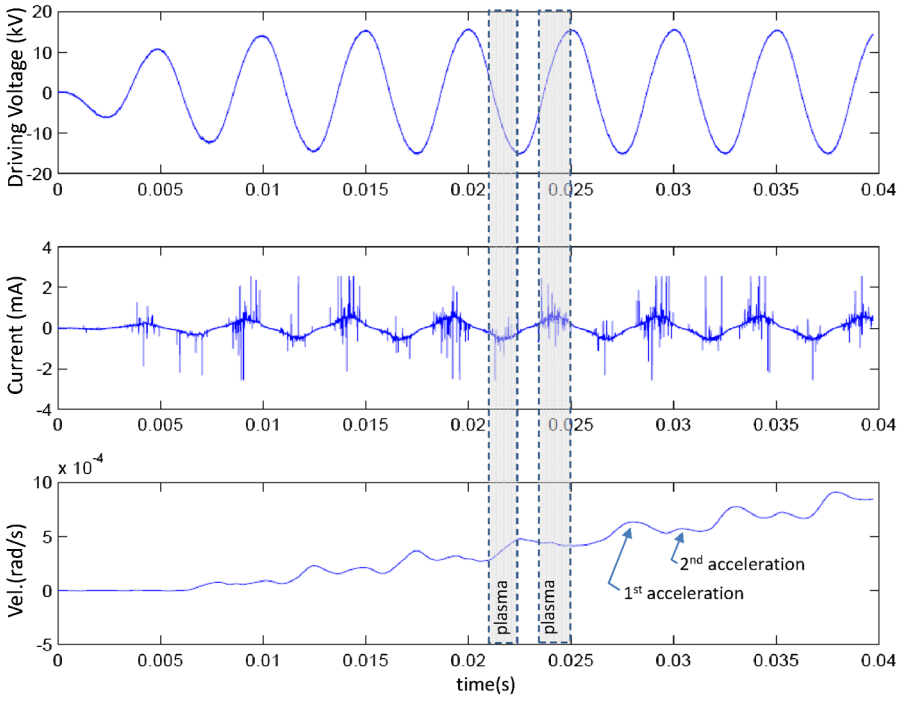

Fig. 6 Driving voltage, plasma current, and derived velocity for a plasma actuator with 20% oxygen mixture.

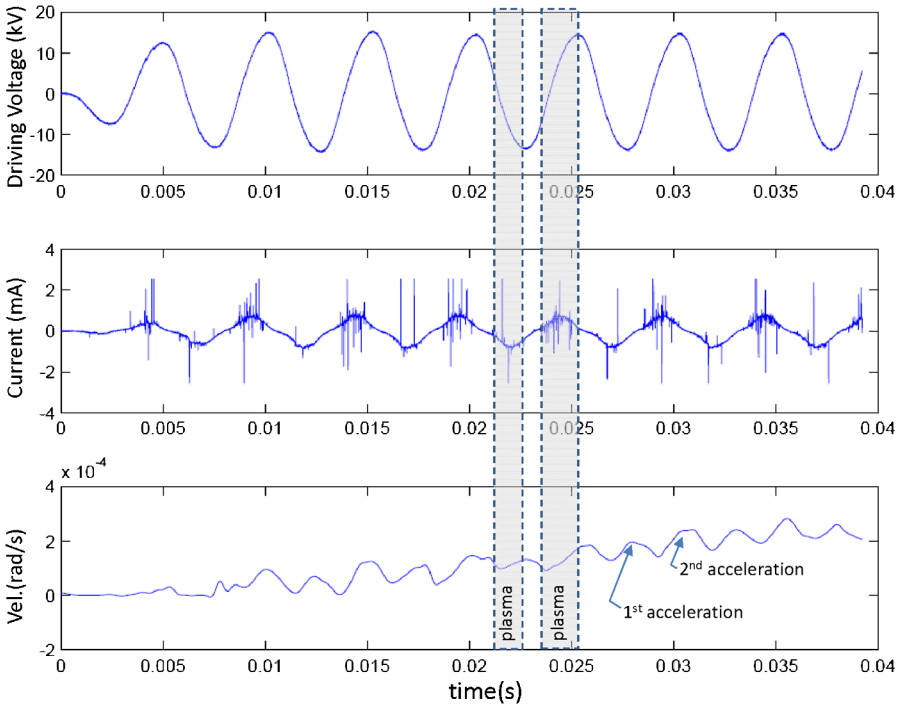

Fig. 7 Measured voltage and current and derived velocity for a plasma actuator with 5% oxygen mixture.

greater than that due to the positive ions. In the 5% O^2 case, the two accelerations are of similar magnitude. Note that as the oxygen content is diminished the velocity of the actuator also decreases, indicating a decrease in the total force imparted by the actuator. In the 20% oxygen case, the actuator achieved a velocity of about 8×10^{-4} rad/s, while in the 5% case the actuator velocity only reaches one quarter of that, about 2×10^{-4} rad/s.

Repeating the experiment for 0% oxygen yields a puzzling result. Figure 8 shows the voltage, current, and velocity for the case where the actuator is run in a pure nitrogen environment. As in previous figures, the two plasma events that occur during a typical AC cycle are highlighted with gray bands. Since nitrogen does not produce negative ions, it was theorized that the velocity trace would display only a single accelerating event per AC cycle. Theoretically, the positive ions should be forced downstream, while the exposed electrode was positive, producing an acceleration of the actuator. Following this, the positive ions should be pulled back, while the exposed electrode was negative, producing a deceleration of the actuator. Instead, as shown by Fig. 8, the trace reveals either two decelerating events or two delayed accelerating events per AC cycle. The reason for this is not clear and this result does not agree with pressure data from [10]. The character of the pressure data in that study, however, was changed markedly by modifying the exposed electrode edge. It is possible that the exposed electrode in the present

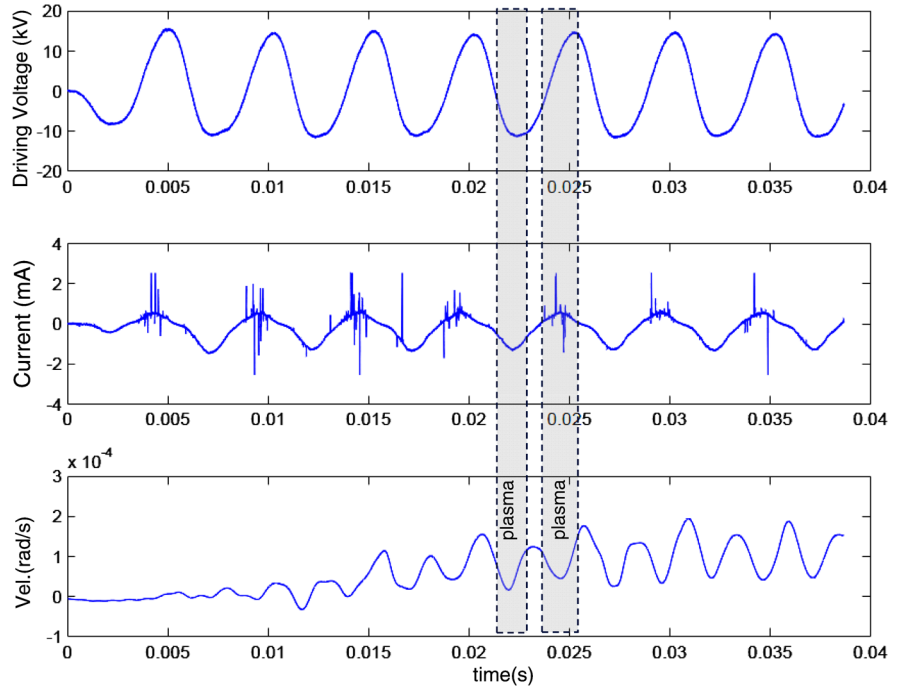

Fig. 8 Measured voltage and current and derived velocity for a plasma actuator in pure nitrogen (0% oxygen mixture).

study has some subtleties in its geometry which is not appreciated. In addition, a couple of factors may be contributing to the present result. The first factor is that the driving voltage is no longer symmetric. (Note that the driving voltage in Fig. 8 oscillates between positive 15 kV and −10 kV.) This occurs because, in the current experimental setup, the plasma is being driven by a step-up transformer and the voltage that eventually appears on the exposed electrode depends, in part, on the impedance of the plasma. The removal of the oxygen appears to have altered the plasma chemistry in a manner that produces significant differences in the impedance of the plasma for each half-cycle resulting in different maximum positive and negative voltages. Circuit element simulations indicate that the degree of asymmetry we observe is consistent with an order of magnitude difference in the impedance between the positive and negative half-cycles, with the positive half-cycle having the larger impedance.

The second factor which may be affecting the force characteristics is the charge buildup on the surface of the dielectric. In previous experiments, it was discovered that the dielectric surface was attaining a positive potential which remained throughout multiple AC cycles [15]. It is possible that the charges on the dielectric surface of an actuator operated in pure nitrogen sufficiently alter the local electric field to produce the observed effects on the temporal force characteristics.

IV. Surface Potential Measurements

In an effort to characterize the surface charging, experiments were run where the charging state of the dielectric surface was measured. The experiments were carried out for cases with 20, 5, and 0% oxygen (pure nitrogen) in the manner described in the methods section above. The driving frequency is maintained at 200 Hz. The results for 20% oxygen are shown in Fig. 9. The driving voltage on the exposed electrode is given by the data at $x = 0.0$ mm. Three trials were conducted at each condition to establish repeatability. The experimental uncertainty in the voltage data is less than ± 0.5 kV.

The data indicate that the closer a station is to the exposed electrode, the more closely it follows the driving voltage. At locations farther away, such as at $x = 11.0$ mm and greater, the voltage on the surface remains positive. It appears that when the actuator is operated in an oxygen rich atmosphere, it creates a region which remains positively charged throughout the discharge. Figure 10 displays the same data as temporal profiles along the surface in the streamwise direction. Eight snapshots at different points during a single bias cycle are displayed. The normalized time for each snapshot is given in the legend. In addition, bold-face numbers label the relative order of the snapshots. The results confirm that at a distance greater than about 10 mm from the exposed electrode, the dielectric surface remains positively charged throughout the discharge. The charging is severe enough, for a 12 kV driving voltage, to build up a 3–7 kV bias 14 mm from the exposed electrode. Experiments run with a 7 kV driving voltage (not shown) acquired a 2–3 kV permanent positive voltage, therefore, the voltage buildup appears to be in the neighborhood of about one third of the driving voltage.

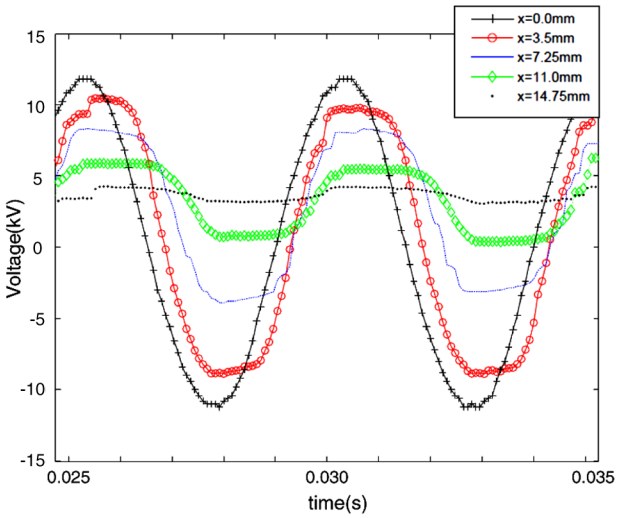

Fig. 9 Measured dielectric surface voltage for an actuator operated in 20% oxygen, 12.5 kV, 200 Hz.

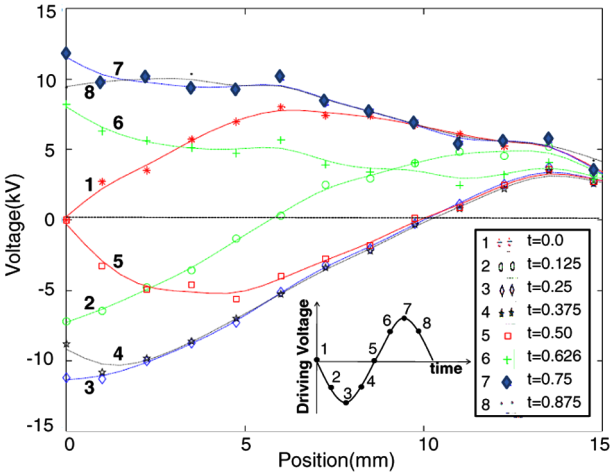

Fig. 10 Measured dielectric surface voltage for an actuator operated in 20% oxygen as a function of distance downstream of exposed electrode (12.5 kV, 200 Hz). Each profile is at the indicated fraction of the bias period.

When the experiments are conducted in an atmosphere containing only 5% oxygen, the results are very similar. Figure 11 shows the dielectric surface voltage profiles for an actuator discharge in 5% oxygen at different points of the bias cycle. As in the previous case, a region of positive voltage is formed at a distance of 11 mm downstream of the exposed electrode. This agrees with the temporal force measurements, which suggested that the discharge characteristics do not appear to change as the oxygen content is lowered from 20 to 5%. For these cases, the discharge is still dominated by the oxygen.

The charging experiments were repeated in a pure nitrogen atmosphere (0% oxygen) for a driving voltage of 12 kV. The voltage on five stations and the driving voltage as a function of time are shown in Fig. 12. The driving voltage is no longer symmetric and now fluctuates between +12 kV and −9 kV. This is due, as mentioned above, to the plasma being driven by a transformer and the changing impedance of the plasma during each half-cycle. Removing the oxygen has a rather dramatic effect on the dielectric

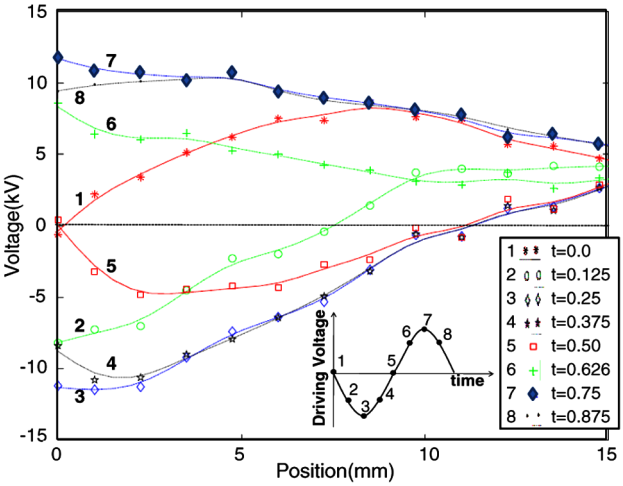

Fig. 11 Measured dielectric surface voltage for an actuator operated in 5% oxygen as a function of distance downstream of exposed electrode (12.5 kV, 200 Hz). Each profile is at the indicated fraction of the bias period.

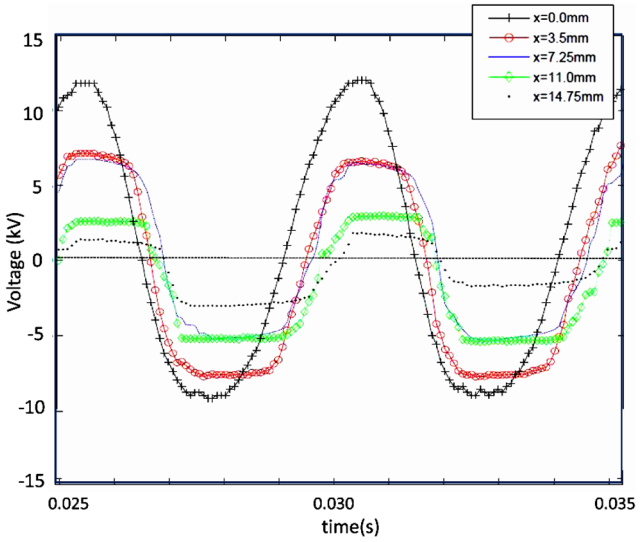

Fig. 12 Measured dielectric surface voltage for an actuator operated in pure nitrogen (0% oxygen, 12.5 kV, 200 Hz).

surface charging pattern. The surface at a large distance from the exposed electrode no longer remains positively charged. Instead, the entire surface alternately biases negatively and positively following the exposed electrode bias.

Figure 13 displays the same data formatted as streamwise profiles at different points during the bias cycle. The data shows that the surface not only is fluctuating between positive and negative but, at large distances from the exposed electrode (>7 mm), the surface remains negative for more than half of the bias cycle. In addition, even though the driving voltage peaks at a larger positive voltage than a negative voltage, the dielectric surface away from the exposed electrode reaches greater negative voltages (−6–−7 kV) than positive voltages (2–3 kV).

The presence of a region on the dielectric dominated, to some extent, by a negative bias, however, does not explain how the plasma in pure nitrogen appears to push twice during a single bias cycle, as was shown in Fig. 8. Perhaps the force imparted to the ions is determined by the electric field closer to the exposed electrode. From the data in Fig. 13, the electric field immediately next to the exposed electrode can be calculated. Figure 14 displays the driving voltage on the exposed electrode, the electric field immediately next to the exposed electrode, and the velocity of the actuator. The two plasma discharges during a single bias cycle (inferred from the plasma

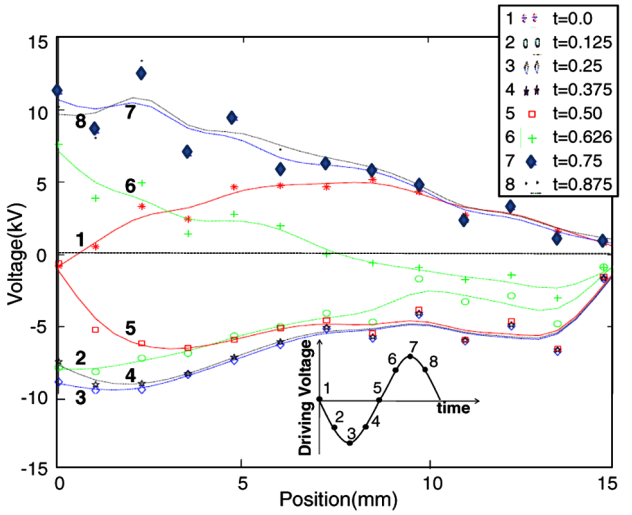

Fig. 13 Measured dielectric surface voltage for an actuator operated in 0% oxygen as a function of distance downstream of exposed electrode. Each profile is at the indicated fraction of the bias period.

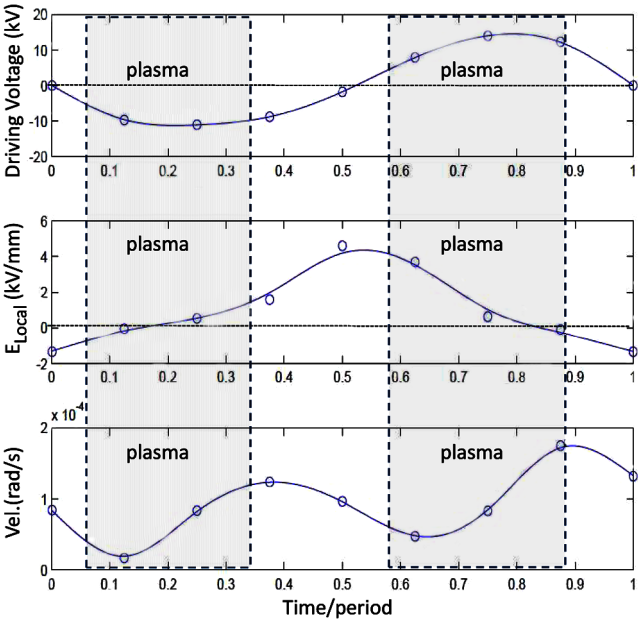

Fig. 14 Driving voltage on the exposed electrode, the electric field within a millimeter of the exposed electrode, and the velocity of the actuator. The two plasma discharges events are indicated by the gray bands (0% oxygen, 200 Hz).

current data) are indicated by the gray bands. Changes in the velocity of the actuator will be used to infer the forces produced by the plasma. The acceleration is, again, not used to determine the force due to excessive noise in the signal.

The results in Fig. 14 show that as the driving voltage on the exposed electrode starts to become negative (time/period = 0.0) the actuator is slowing down. Since plasma is not yet present, this deceleration is most likely due to fluid drag. As the plasma ignites the positive ions are pulled back by the negative local electric field. This causes further deceleration of the actuator. At a normalized time of about 0.15, however, the local electric field begins to become positive. Note that this occurs even though the exposed electrode (driving voltage) is still negative. This can also be seen on Fig. 13, where by profile #2, the voltage is unchanging in the first millimeter (negligible electric field) and by profile #3, the potential at 1 mm is lower than at 0 mm (positive electric field). This positive electric field forces ions away from the exposed electrode resulting in a negative electrode *repelling* positive ions and producing a positive force. By the normalized time of 0.35 the plasma extinguishes and the positive force vanishes. At this point, the velocity ceases to increase (due to a lack of plasma force) and the subsequent fluid drag begins to decelerate the actuator. Between the normalized times of 0.35 and 0.58, the local electric field soars to 4 kV/mm because there are no new charges to land on the dielectric surface and cancel the local electric field. At normalized time 0.58 the plasma reignites and but does not appear to grow dense enough to generate a force sufficiently large to cancel the fluid drag until a normalized time of about 0.63. After this the actuator accelerates due to the positive force created by the positive ions in a positive electric field until a normalized time of nearly 0.9. Note that after this, the local electric field becomes negative, even though the exposed electrode is still positive. The plasma has extinguished by this time, however, and the actuator deceleration must, again, be due to fluid drag. The results suggest, therefore, that a nitrogen plasma, which produces only positive ions, can indeed produce two pushes (accelerations). One is easy to understand because the exposed electrode is positive and it pushes ions away. The other push appears to be due to the effect of the surface charging. The electric field immediately next to the exposed electrode during the negative part of the bias cycle can become positive for a sufficiently long extent of time to create a push (positive force) to the positive ions.

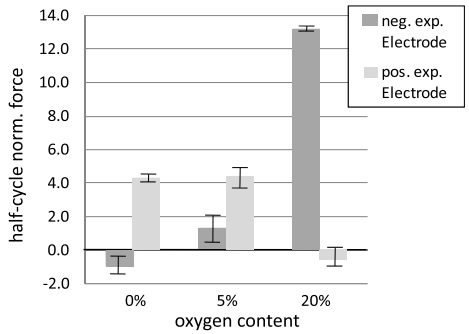

Fig. 15 Net normalized force (plasma and fluid) for each half of bias cycle as a function of oxygen content.

It is interesting to compare the different contributions to the total actuator force provided by each half of the bias cycle. This includes, not only the force provided by the plasma as detailed above, but also the force provided by the fluid drag on the actuator. Figure 15 separates the total force into that imparted while the exposed electrode is negative and while it is positive. In the figure, the force is normalized by value from the negative half-cycle of the 0% oxygen case.

In air (20% oxygen), the actuator produces the previously measured result [4,13] where most of the force is provided when the exposed electrode is negative. The positive half-cycle appears to produce a small net negative force when the fluid drag is included, but this result is within the scatter of the data and may not be statistically significant. As the oxygen content is lowered to 5%, the positive half of the bias cycle results in about four times more momentum addition to the air than the negative half-cycle. When the oxygen is completely removed, the negative half-cycle provides a net negative force. Even though the temporal data shown above indicated that the negative half-cycle for the 0% oxygen case was providing some amount of positive force, it appears that the fluid drag more than cancels this out. This negative force, unlike the 20% O_2 case, is significant as it is larger than the scatter in the data.

V. Conclusions

Experiments have been conducted on a plasma actuator in a nitrogen-oxygen environment where the amount of oxygen relative to the nitrogen was varied. The effects of varying oxygen on temporal force production characteristics and dielectric surface charging were measured using interferometry and split electrode techniques. The results reveal that oxygen appears to be the main contributor to total force production. As the amount of oxygen decreases, the total force also decreases until the oxygen content is about 5%. At smaller oxygen content amounts, the force production remains more steady and appears to be dominated by the nitrogen. Temporal force measurements show that the actuator accelerates the air downstream twice during each bias cycle. This is maintained at all oxygen content levels, although the size of the force produced by the positive half-cycle relative to the negative half-cycle changes as the oxygen content level changes. Most surprising, the actuator continues to have two downstream accelerating events per bias cycle even in the absence of all oxygen. This was shown to be made possible by the electric field in the immediate vicinity of the exposed electrode, which was being altered by dielectric surface charging. Measurements of the dielectric surface charging also revealed that, in the presence of oxygen, the actuator builds up a large positive voltage in the order of thousands of volts downstream of the exposed electrode. In the absence of oxygen, no such region is created and the dielectric alternates between positive and negative voltage. Away from the exposed electrode, the dielectric, in the absence of oxygen, spends the majority of the bias cycle with a negative voltage. Finally, at high oxygen content levels, most of the force is produced during the time that the exposed electrode is negative. As the oxygen level drops, the amount of force produced during the negative half-cycle decreases and the majority of the force is produced during the positive half-cycle. In the absence of oxygen, the negative half-cycle produces a net upstream (negative) force that decelerates the flow.

References

[1] Roth, J. R., Sherman, D. M., and Wilkinson, S. P., "Electrohydrodynamic Flow Control with a Glow-Discharge Surface Plasma," *AIAA Journal*, Vol. 38, No. 7, 2000, pp. 1166–1172. doi:10.2514/2.1110

[2] Post, M. L., and Corke, T. C., "Separation Control Using Plasma Actuators: Dynamic Stall Vortex Control on Oscillating Airfoil," *AIAA Journal*, Vol. 44, No. 12, 2006, pp. 3125–3135. doi:10.2514/1.22716

[3] Moreau, E., "Airflow Control by Non-Thermal Plasma Actuators," *Journal of Physics D: Applied Physics*, Vol. 40, No. 3, 2007, pp. 605–636. doi:10.1088/0022-3727/40/3/S01

[4] Forte, M., Jolibois, J., Pons, J., Moreau, E., Touchard, G., and Cazalens, M., "Optimization of a Dielectric Barrier Discharge Actuator by Stationary and Non-Stationary Measurements of Induced Flow Velocity: Application to Airflow Control," *Experiments in Fluids*, Vol. 43, No. 6, 2007, pp. 917–928. doi:10.1007/s00348-007-0362-7

[5] Borghi, C. A., Carraro, M. R., Cristofolini, A., and Neretti, G., "Electrohydrodynamic Interaction Induced by a Dielectric Barrier Discharge," *Journal of Applied Physics*, Vol. 103, No. 6, 2008, p. 063304. doi:10.1063/1.2888354

[6] Opaits, D. F., Likhanskii, A. V., Neretti, G., Zaidi, S., Shneider, M. N., Miles, R. B., and Macheret, S. O., "Experimental Investigation of Dielectric Barrier Discharge Plasma Actuators Driven by Repetitive High-Voltage Nanosecond Pulses with DC or Low Frequency Sinusoidal Bias," *Journal of Applied Physics*, Vol. 104, No. 4, 2008, p. 043304. doi:10.1063/1.2968251

[7] Opaits, D. F., Shneider, M. N., Miles, R. B., Likhanskii, A. V., and Macheret, S. O., "Surface Charge in Dielectric Barrier Discharge Plasma Actuators," *Physics of Plasmas*, Vol. 15, No. 7, 2008, p. 073505. doi:10.1063/1.2955767

[8] Likhanskii, A. V., Shneider, M. N., Macheret, S. O., and Miles, R. B., "Modeling of Dielectric Barrier Discharge Plasma Actuator in Air," *Journal of Applied Physics*, Vol. 103, No. 5, 2008, p. 053305. doi:10.1063/1.2837890

[9] Kim, W., Do, H., Mungal, M. G., and Cappelli, M. A., "On the Role of Oxygen in Dielectric Barrier Discharge Actuation of Aerodynamic Flows," *Applied Physics Letters*, Vol. 91, No. 18, 2007, p. 181501. doi:10.1063/1.2803755

[10] Leonov, S., Opaits, D. F., Miles, R. B., and Soloviev, V., "Time-Resolved Measurements of Plasma-Induced Momentum in Air and Nitrogen Under DBD Actuation," *Physics of Plasmas*, Vol. 17, No. 11, 2010, p. 113505. doi:10.1063/1.3494279

[11] Boeuf, J. P., Lagmich, Y., and Pitchford, L. C., "Contribution of Positive and Negative Ions to the Electrohydrodynamic Force in a Dielectric Barrier Discharge Plasma Actuator Operating in Air," *Journal of Applied Physics*, Vol. 106, No. 2, 2009, p. 023115. doi:10.1063/1.3183960

[12] Benard, N., and Moreau, E., "Capabilities of the Dielectric Barrier Discharge Plasma Actuator for Multi-Frequency Excitations," *Journal of Physics D: Applied Physics*, Vol. 43, No. 14, 2010, p. 145201. doi:10.1088/0022-3727/43/14/145201

[13] Enloe, C. L., McHarg, M. G., and McLaughlin, T. E., "Time-Correlated Force Production Measurements of the Dielectric Barrier Discharge Plasma Aerodynamic Actuator," *Journal of Applied Physics*, Vol. 103, No. 7, 2008, pp. 073302–073307. doi:10.1063/1.2896590

[14] Enloe, C. L., McHarg, M. G., Font, G. I., and McLaughlin, T. E., "Plasma-Induced Force and Self-induced Drag in the Dielectric Barrier Discharge Aerodynamic Plasma Actuator," AIAA Paper 2009-1622, 2009.

[15] Enloe, C. L., Font, G. I., McLaughlin, T. E., and Orlov, D., "Surface Potential and Longitudinal Electric Field Measurements in the Aerodynamic Plasma Acuator," *AIAA Journal*, Vol. 46, No. 11, 2008, pp. 2730–2740. doi:10.2514/1.33973

[16] Enloe, C. L., McLaughlin, T. E., Font, G. I., and Baughn, J. W., "Parameterization of Temporal Structure in the Single Dielectric Barrier

Aerodynamic Plasma Actuator," *AIAA Journal*, Vol. 44, No. 6, 2006, pp. 1127–1136.
doi:10.2514/1.16297

[17] Kossyi, I. A., Kostinsky, A. Y., Matveyev, A. A., and Silakov, V. P., "Kinetic Scheme of the Non-Equilibrium Discharge in Nitrogen-Oxygen Mixtures," *Plasma Sources Science and Technology* , Vol. 1, No. 3, 1992, pp. 207–220.
doi:10.1088/0963-0252/1/3/011

[18] Font, G. I., Enloe, C. L., and McLaughlin, T. E., "Plasma Volumetric Effects on the Force Production of a Plasma Actuator," *AIAA Journal*, Vol. 48, No. 9, 2010, pp. 1869–1874.
doi:10.2514/1.J050003

M. Visbal
Associate Editor